Analytica Chimica Acta 814 (2014) 23–30

Contents lists available at ScienceDirect

Analytica Chimica Acta

journal homepage: www.elsevier.com/locate/aca

Determination of five pesticides in juice, fruit and vegetable samples by means of liquid chromatography combined with multivariate curve resolution

Valeria Boeris, Juan A. Arancibia, Alejandro C. Olivieri *

Departamento de Química Analítica, Facultad de Ciencias Bioquímicas y Farmacéuticas, Universidad Nacional de Rosario e Instituto de Química Rosario (IQUIR-CONICET), Suipacha 531, S2002LRK Rosario, Argentina

HIGHLIGHTS

- Five pesticides were determined in juice, fruit and vegetable samples.
- Liquid chromatography was coupled to diode array detection.
- Chromatographic-spectral matrices were analyzed by multivariate curve resolution.

GRAPHICAL ABSTRACT

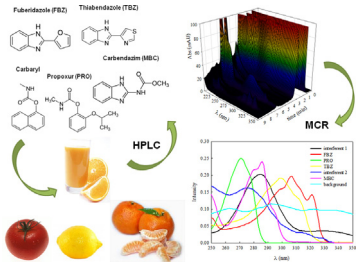

ARTICLE INFO

Article history:
Received 11 November 2013
Received in revised form 4 January 2014
Accepted 10 January 2014
Available online 18 January 2014

Keywords:
High-performance liquid chromatography
Diode array detection
Multivariate curve resolution
Pesticides
Vegetable samples

ABSTRACT

The aim of this work was to quantify five commonly used pesticides (propoxur, carbaryl, carbendazim, thiabendazole and fuberidazole) in real samples as: tomato, orange juice, grapefruit juice, lemon and tangerine. The method used for the determination of these analytes in the complex matrices was high-performance liquid chromatography with diode array detection. In order to work under isocratic conditions and to complete each run in less than 10 min, the analysis was carried out applying multivariate curve resolution coupled to alternating least-squares (MCR–ALS). The flexibility of this applied multivariate model allowed the prediction of the concentrations of the five analytes in complex samples including strongly coeluting analytes, elution time shifts, band shape changes and presence of uncalibrated interferents. The obtained limits of detection (in $\mu g\,L^{-1}$) using the proposed methodology were 2.3 (carbendazim), 0.90 (thiabendazole), 12 (propoxur), 0.46 (fuberidazole) and 0.32 (carbaryl).

© 2014 Elsevier B.V. All rights reserved.

1. Introduction

Although the use of pesticides provides unquestionable benefits in providing a plentiful, low-cost supply of high-quality fruits and vegetables, their incorrect application may leave harmful residues, which involve possible health risk [1]. The concentration of pesticides is regulated in many samples such as drinking waters, vegetables, juices, etc., by the European Commission [2] and the Food and Drug Administration [3], among other agencies. Traditionally, the instrumental techniques employed to determine these compounds involve fluorescence, gas or liquid chromatography [4–8]. Specifically, the determination of benzimidazolic pesticides (carbendazim, thiabendazole and fuberidazole) and/or carbamates (carbaryl, propoxur and carbendazim) in fruits and vegetables have been carried out by various approaches, such as supramolecular solvent-based microextraction followed by high-performance

Abbreviations: HPLC, high-performance liquid chromatography; DAD, diode array detection; MCR–ALS, multivariate curve resolution coupled to alternating least-squares; PRO, propoxur; CBL, carbaryl; MBC, carbendazim; TBZ, thiabendazole; FBZ, fuberidazole.

* Corresponding author. Tel.: +54 3414372704; fax: +54 3414372704.
E-mail addresses: olivieri@iquir-conicet.gov.ar, aolivier@fbioyf.unr.edu.ar (A.C. Olivieri).

0003-2670/$ – see front matter © 2014 Elsevier B.V. All rights reserved.
http://dx.doi.org/10.1016/j.aca.2014.01.034

liquid chromatography (HPLC) with fluorescence detection [9], gas chromatography coupled to mass spectrometry and selected ion monitoring [10], enzymatic immunoassay using antibodies [11–13] or electrochemical methods [14,15].

The analysis of mixtures of pesticides using methods based on HPLC sometimes results in complex separations and overlapped peaks [16,17]. Nevertheless, complex multicomponent mixtures can in many cases be qualitatively and quantitatively resolved by means of chemometrics. Depending on their nature, data can be arranged in a two-way structure (a table or a matrix), as in the case of collecting the absorbance spectra for many samples, or in a three-way structure, e.g., in HPLC with diode array detection (DAD), where spectra are recorded at several elution times for each sample. Such data arrangements in three- or higher way arrays can be handled using multi-way methods of analysis [18,19].

Collection of multi-dimensional chromatographic information, and data processing by advanced chemometric algorithms constitute a fruitful combination of techniques, recently applied to diverse research areas [20–22]. Chemometrics is required whenever perfect separation of the various sample components cannot be achieved by the employed chromatographic system, leading to overlapping peaks in the elution time mode. In these cases, selectivity may be mathematically restored by applying multivariate data analysis [23]. In particular, the so-called second-order advantage can be achieved, a property which is inherent to matrix instrumental data, and implies that analytes can be quantified in samples containing potential interferences [21]. Signals arising from coeluting analytes or foreign components can be modeled by powerful second-order multivariate algorithms.

The combination of chemometrics to HPLC presents additional advantages in relation to traditional methods: since chemometrics allows resolving coeluted peaks, it is possible to reduce the duration of the chromatographic run, allowing not only processing more samples but also reducing the solvent consumption, saving time and money. Moreover, several authors report that gradient of solvents was required to achieve resolution of the analytes [24–26]: this requirement may be avoided using isocratic conditions and resolving the peak by applying chemometrics.

In liquid chromatographic runs, elution time shifts and band shape changes usually occur from sample to sample: in these cases, a useful alternative is to analyze the data with flexible algorithms, which allow a given component to present different time profiles in different samples, such as parallel factor analysis 2 (PARAFAC2) or multivariate curve resolution coupled to alternating least-squares (MCR–ALS) [27]. Recent work from our laboratory indicated better performance with MCR–ALS in the case of multi-analyte quantification in the presence of high overlapping of elution profiles and uncalibrated interferences, mainly because of the possibility of building a more constrained model in MCR–ALS in comparison with PARAFAC2 [22].

In the present report, we selected MCR–ALS as the algorithm of choice for processing HPLC–DAD data, and discuss its behavior towards the quantification of the following five pesticides in fruit and vegetable samples: propoxur (PRO), carbaryl (CBL), carbendazim (MBC), thiabendazole (TBZ) and fuberidazole (FBZ) (Fig. 1). The presence of benzimidazoles, carbamates and their degradation products in waters or food products is potentially harmful for humans due to their proven toxicity. This is the cause of the continued interest in the development of analytical methods for monitoring these families of compounds. Previous chromatographic analysis of the presently studied compounds required up to 35 min [28,29]. The aim of this work is to quantify these analytes in complex matrices under HPLC isocratic conditions and in less than 10 min.

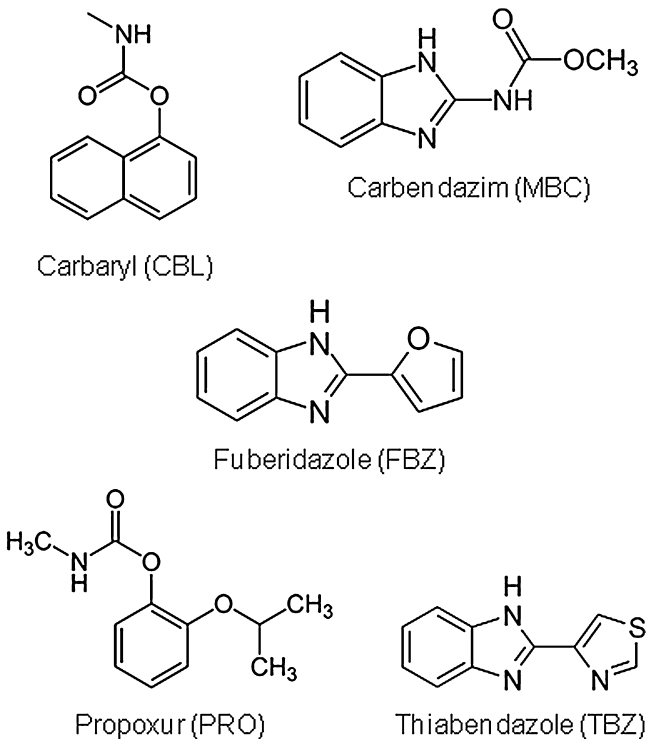

Fig. 1. Chemical structures of the five assayed pesticides.

2. Theory

The bilinear model assumed by MCR methods is analogous to the generalized Lambert–Beer's law, where the individual responses of each component are additive. In matrix form, this bilinear model is expressed as:

$$\mathbf{D} = \mathbf{C}\mathbf{S}^{\mathrm{T}} + \mathbf{E} \tag{1}$$

where $\mathbf{D}$ (size $J \times K$) is the matrix of experimental data (J is the number of elution time data points and K is the number of absorption wavelengths), $\mathbf{C}$ (size $J \times N$) is the matrix whose columns contain the concentration profiles of the N components present in the samples, $\mathbf{S}^{\mathrm{T}}$ (size $N \times K$) is the matrix whose rows contain the component spectra and $\mathbf{E}$ (size $J \times K$) is a matrix collecting the experimental error and the variance not explained by the bilinear model of Eq. (1).

The first step in MCR–ALS studies is to obtain a rough estimation of the number of components, which can be simply performed by visual inspection of singular values or principal component analysis (PCA) [30,31].

The resolution is accomplished using an iterative ALS procedure, initialized using an initial estimation of the spectral or concentration profiles for each intervening species. Different methods are used for this purpose, such as evolving factor analysis [32] or the determination of the purest variables [33]. If the initial estimations are the spectral profiles, the unconstrained least-squares solution for the concentration profiles can be calculated from the expression:

$$\mathbf{C} = \mathbf{D}(\mathbf{S}^{\mathrm{T}})^{+} \tag{2}$$

where $(\mathbf{S}^{\mathrm{T}})^{+}$ is the pseudoinverse of the spectral matrix $\mathbf{S}^{\mathrm{T}}$ [34]. If the initial estimations were the concentration profiles, the unconstrained least-squares solution for the spectra can be calculated from the expression:

$$\mathbf{S}^{\mathrm{T}} = \mathbf{C}^{+}\mathbf{D} \tag{3}$$

where $\mathbf{C}^+$ is the pseudoinverse of $\mathbf{C}$. Both steps can be implemented in an alternating least-squares cycle, so that, at each iteration, new $\mathbf{C}$ and $\mathbf{S}^T$ matrices are obtained. During these iterative recalculations of $\mathbf{C}$ and $\mathbf{S}^T$, a series of constraints (e.g., non-negativity, unimodality and sample selectivity; the latter removes a component which is known to be absent in a given sample) could be applied to give physical meaning to the obtained solutions, and to limit their possible number for the same data fitting and decrease the extent of possible rotation ambiguities [35]. Iterations continue until an optimal solution is obtained that fulfils the postulated constraints and the established convergence criteria.

The procedure described above can be easily extended to the simultaneous analysis of multiple data sets or data matrices if they have at least one data mode (direction) in common. For instance, if the different data sets have been analyzed by the same spectroscopic method, the possible data arrangement and bilinear model extension is given by the following equation:

$$\mathbf{D}_{aug} = \begin{bmatrix} \mathbf{D}_{cal1} \\ \mathbf{D}_{cal2} \\ \cdots \\ \mathbf{D}_{test} \end{bmatrix} = \begin{bmatrix} \mathbf{C}_{cal1} \\ \mathbf{C}_{cal2} \\ \cdots \\ \mathbf{C}_{test} \end{bmatrix} \mathbf{S}^T + \begin{bmatrix} \mathbf{E}_{cal1} \\ \mathbf{E}_{cal2} \\ \cdots \\ \mathbf{E}_{test} \end{bmatrix} = \mathbf{C}_{aug}\mathbf{S}^T + \mathbf{E}_{aug} \quad (4)$$

where $\mathbf{D}_{aug}$ is the augmented data matrix, constructed from I individual data matrices [36], corresponding to the set of calibration samples ($\mathbf{D}_{cal1}$, $\mathbf{D}_{cal2}$, ...) and to a single test sample ($\mathbf{D}_{test}$).

In this case, $\mathbf{C}_{aug}$ is the column-wise augmented matrix of concentration profiles (size $JI \times N$, where N is the number of responsive chemical components), $\mathbf{S}^T$ is the matrix of loadings (dimensions $N \times K$) in the row vector space, and $\mathbf{E}_{aug}$ collects the residuals. After decomposition, the scores for analyte n are computed as the sum of the elements of the corresponding profile in each of the submatrices of $\mathbf{C}_{aug}$.

Finally, the calibration scores are employed to build a pseudo-univariate calibration line, leading to an estimation of the corresponding slope (m_n) and offset (n_n). The analyte score in the test sample is then interpolated in the calibration line to yield the predicted analyte concentration c_n:

$$c_n = \frac{(a_{test,n} - n_n)}{m_n} \quad (5)$$

3. Experimental

3.1. Reagents

Carbendazim (MBC), thiabendazole (TBZ), fuberidazole (FBZ), propoxur (PRO) and carbaryl (CBL) were purchased from Sigma Aldrich Co. (St. Louis, MO). Methanol was obtained from Merck. Milli-Q water (Millipore) was used in all experiments. Solvents were filtered through 0.45 μm filters.

3.2. Stock standard and working standard solutions

Stock standard solutions of MBC (570 mg L^{-1}), TBZ (1150 mg L^{-1}), FBZ (620 mg L^{-1}), PRO (1720 mg L^{-1}) and CBL (680 mg L^{-1}) were prepared in 25.00 mL volumetric flasks by dissolving accurately weighed amounts of the drugs in methanol and completing to the mark with the same solvent. From these solutions, more diluted solutions were obtained (MBC 22.8 mg L^{-1}, TBZ 20.7 mg L^{-1}, FBZ 9.92 mg L^{-1}, PRO 172 mg L^{-1}, CBL 13.6 mg L^{-1}). Working solutions were prepared immediately before their use by taking appropriate aliquots of solutions and diluting with methanol and water (50:50 v/v) to the desired concentrations.

3.3. Apparatus

Chromatographic runs were performed on an HP 1200 liquid chromatograph (Agilent Technologies, Waldbronn, Germany) consisting of a quaternary pump, a manual injector fitted with a 200 μL loop and a diode array UV–visible detector set at a wavelength range from 200 to 350 nm. A C18 column of 150 mm × 4.6 mm, 5 μm particle size was employed (Agilent Sorbax SB). The data were collected using the software HP ChemStation for LC Rev.HP 1990–1997.

3.4. Software

The data were handled using the MATLAB computer environment [37]. The calculations involved in the mixture resolution by MCR–ALS have been made using mvc2_gui, a MATLAB graphical interface toolbox which is a new version of that already reported in the literature [38].

3.5. Calibration and validation samples

In order to design the calibration set, preliminary experiments were performed with the pure analytes, showing that the full elution time range could be divided into three relevant regions: an overlapped zone where three analytes appear (TBZ, PRO and FBZ) and two regions where the remaining two analytes are fully resolved (MBC and CRL). A set of 18 calibration solutions containing the analytes in the ranges 0–228 μg L^{-1} for MBC, 0–207 μg L^{-1} for TBZ, 0–1720 μg L^{-1} for PRO, 0–99.2 μg L^{-1} for FBZ and 0–136 μg L^{-1} for CBL were prepared in appropriate volumetric flasks. The concentrations are collected in Table 1. Fifteen of these samples correspond to the concentrations provided by a central composite design for the three analytes appearing in the overlapped region: TBZ, PRO and FBZ. Each of the remaining three samples of the 18-sample set corresponds to each of the three pure analytes at their maximum levels. Each of these 18 samples was combined with nine equally spaced, duplicate concentration levels for the two resolved analytes. For establishing the calibration concentration ranges, the linear range for all components was studied by analyzing different solutions covering the interval 0–2000 μg L^{-1}.

A validation set of 10 samples was also prepared, containing the five analytes in concentrations different than those used for calibration, and following a random design, i.e., the specific concentrations were taken as random numbers generated within the calibration domain.

Table 1
Calibration concentrations (μg L^{-1}) for the five assayed analytes.

Sample	MBC	TBZ	PRO	FBZ	CBL
1	0.0	62.1	1376	79.4	136.0
2	0.0	165.6	1376	79.4	122.4
3	22.8	62.1	516	79.4	102.0
4	22.8	165.6	516	29.8	81.6
5	57.0	165.6	1376	29.8	68.0
6	57.0	62.1	1376	29.8	54.4
7	91.2	113.8	172	54.6	34.0
8	91.2	113.8	946	9.9	13.6
9	114.0	113.8	1720	54.6	0.0
10	114.0	165.6	516	79.4	136.0
11	136.8	113.8	946	54.6	122.4
12	136.8	207.0	946	54.6	102.0
13	171.0	20.7	946	54.6	81.6
14	171.0	113.8	946	99.2	68.0
15	205.2	62.1	516	29.8	54.4
16	205.2	207.0	0	0.0	34.0
17	228.0	0.0	1720	0.0	13.6
18	228.0	0.0	0	99.2	0.0

3.6. Samples and sample preparation

Tangerine, lemon, tomato and commercially available orange and grapefruit juice were purchased from local supermarkets. The fruits and vegetables were chopped into small pieces and processed. Accurately weighted portions of fruits and vegetable samples and aliquots of juice samples were spiked with the assayed pesticides. The semi-solid samples (processed tangerine, lemon and tomato) were blended with water. The pH of the pesticides-spiked samples was adjusted to neutral by addition of a solution of NaOH. Each sample was centrifuged for 10 min at 4000*g*, the supernatant was diluted with methanol and the sample was centrifuged again in the same conditions. Finally, each sample was filtered twice prior to injection: first through a 0.45 μm nylon filter and then through a 0.22 μm nylon filter.

3.7. HPLC procedure

The data matrices were collected using wavelengths from 200 to 350 nm each 1 nm, and each 1.6 s in the elution time axis. The slit width was 1 nm. The time-absorption matrices were of size 356×151 and were saved in ASCII format, and transferred to a PC for subsequent manipulation.

The mobile phase used for all chromatographic runs was a 50:50 (v/v) mixture of water and methanol, delivered at a flow rate of 1.0 mL min^{-1} with a chromatographic system operating under isocratic mode. Each chromatogram was accomplished in 9.5 min.

4. Results and discussion

4.1. Analysis of the calibration set

Using pure analyte standards, a chromatographic method allowing their partial separation was developed, making proper selection of the range of detected wavelengths and the composition of the mobile phase, in order to obtain an overall chromatographic time of less than 10 min. Under these conditions, when calibration samples were eluted, a cluster of coeluting peaks and two individual, fully resolved peaks appeared in all chromatographic runs (Fig. 2). Specifically, the MCR–ALS algorithm was used to process LC–DAD matrices taken at specific elution time ranges. Each chromatographic data matrix was divided in the following time regions: region I (3.3–6.9 min) and region II (7.3–9.5 min). These regions were delimited taking into account the spectrum of each analyte (Fig. 3), i.e., the wavelength ranges required to resolve them. Region I includes the four first eluted analytes: MBC, TBZ, PRO and FBZ. The spectrum of these analytes show that the high sensitivity range is from 250 to 350 nm, thus the wavelength range from 200 to 249 nm was discarded in their analysis. However, region II includes the last eluted analyte, CBL, whose maximum absorption peak is at 220 nm. In this region, the full wavelength range was selected.

Notice in Fig. 2 that the analyte elution time profiles significantly shift from run to run. This effect, combined with the presence of potential interferents in some of the analyzed samples, makes it difficult to align the chromatograms in the time mode, in order to restore the trilinearity required by some second-order multivariate algorithms. This is the main reason for employing the MCR–ALS algorithm for data processing. For each time region, MCR–ALS was applied to augmented matrices in the elution time direction, corresponding to the simultaneous analysis of the HPLC–DAD data matrices for the calibration set of samples. In this analysis, initialization of the multivariate algorithm was performed using spectral estimates obtained from the analysis of the purest variables. Non-negativity restriction was applied in both modes; unimodality restriction was applied in the elution time mode only to the signals

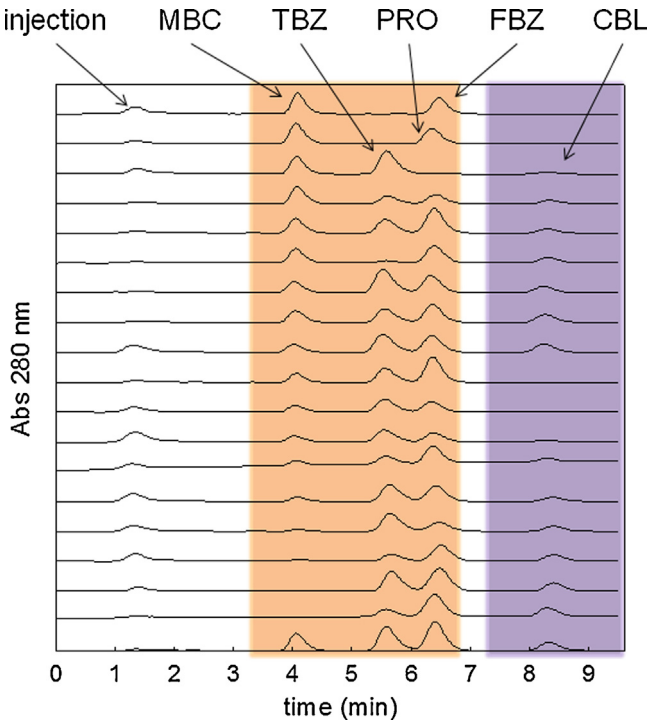

Fig. 2. Liquid chromatograms (λ of detection: 280 nm) for the set of calibration samples. The signal corresponding to each analyte was identified. The subregions selected are highlighted.

corresponding to the analytes (not to the background signal) but correspondence restriction was not applied during the ALS optimization phase.

The number of components was estimated by means of principal component analysis (PCA). The estimated number of components was five in region I and two in region II, which can be justified taking into account the presence of five different signals (corresponding to MBC, TBZ, PRO, FBZ and a background signal) in region I and two different signals (corresponding to CBL and a background signal) in region II. The resolution of calibration samples provided the characteristic chromatographic profiles and pure spectra for the different analytes plus one signal corresponding to a background. The number of iterations was less than 10 in all cases, with a residual fit lower than 0.07 mUA (region I) and 0.1 mUA (region II). Both

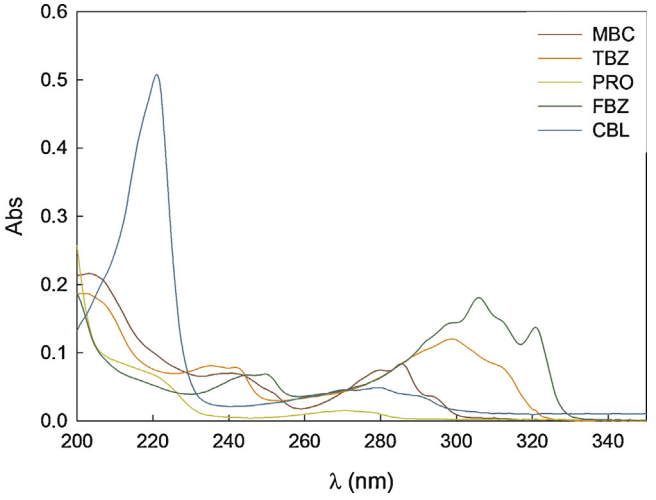

Fig. 3. Spectra of pure standards of the five assayed pesticides in medium methanol-water (50:50 v/v). Pesticide concentration: 1 mg L^{-1}.

residual fits are on the order of the expected instrumental noise associated with DAD detection.

After MCR–ALS resolution of the augmented calibration matrix, a pseudo-univariate calibration was carried out for each compound. The parameters corresponding to the linear regression of the scores from Eq. (5) vs. the corresponding nominal concentrations are shown in Table 2.

Region I corresponds to the fully overlapped peaks for PRO and FBZ, the partially overlapped peak for TBZ and also to the isolated peak for MBC (Fig. 4A). Five different independent contributions were resolved by MCR–ALS in the first peak cluster, corresponding to region I (Fig. 4A). For a typical sample, the five MCR–ALS resolved elution profiles are shown in Fig. 4B, and the spectra (common to all samples) in Fig. 4C. These five contributions were identified as the analytes MBC, TBZ, PRO, FBZ and a background signal by comparison of the MCR-obtained spectra with the actual spectra of the pure compounds (Fig. 3). Coelutions shown in Fig. 4A are untreatable by traditional chromatography; however, mathematical resolution using MCR–ALS was still possible by processing second-order HPLC–DAD data.

Table 2
Summary of the results from the pseudo-univariate calibration curves for all analytes[a].

	Slope[b]	Intercept[b]	r^2	$s_{y/x}$	p Value
MBC	1.48 (3)	−2 (4)	0.9833	14	0.161
TBZ	5.16 (7)	11 (9)	0.9894	29	0.464
PRO	0.252 (4)	7 (4)	0.9917	13	0.603
FBZ	9.8 (2)	20 (10)	0.9894	33	0.262
CBL	12.0 (2)	−10 (10)	0.9902	56	0.253

[a] r^2, squared correlation coefficient; $s_{y/x}$, standard deviation of regression residuals, p value, probability associated to the IUPAC recommended F test for linearity ($p > 0.05$ implies linearity at 95% confidence level).
[b] Standard deviation in parenthesis.

Region II contained a fully resolved peak at 8.3 min belonging to CBL. The analysis of CBL was done both by the

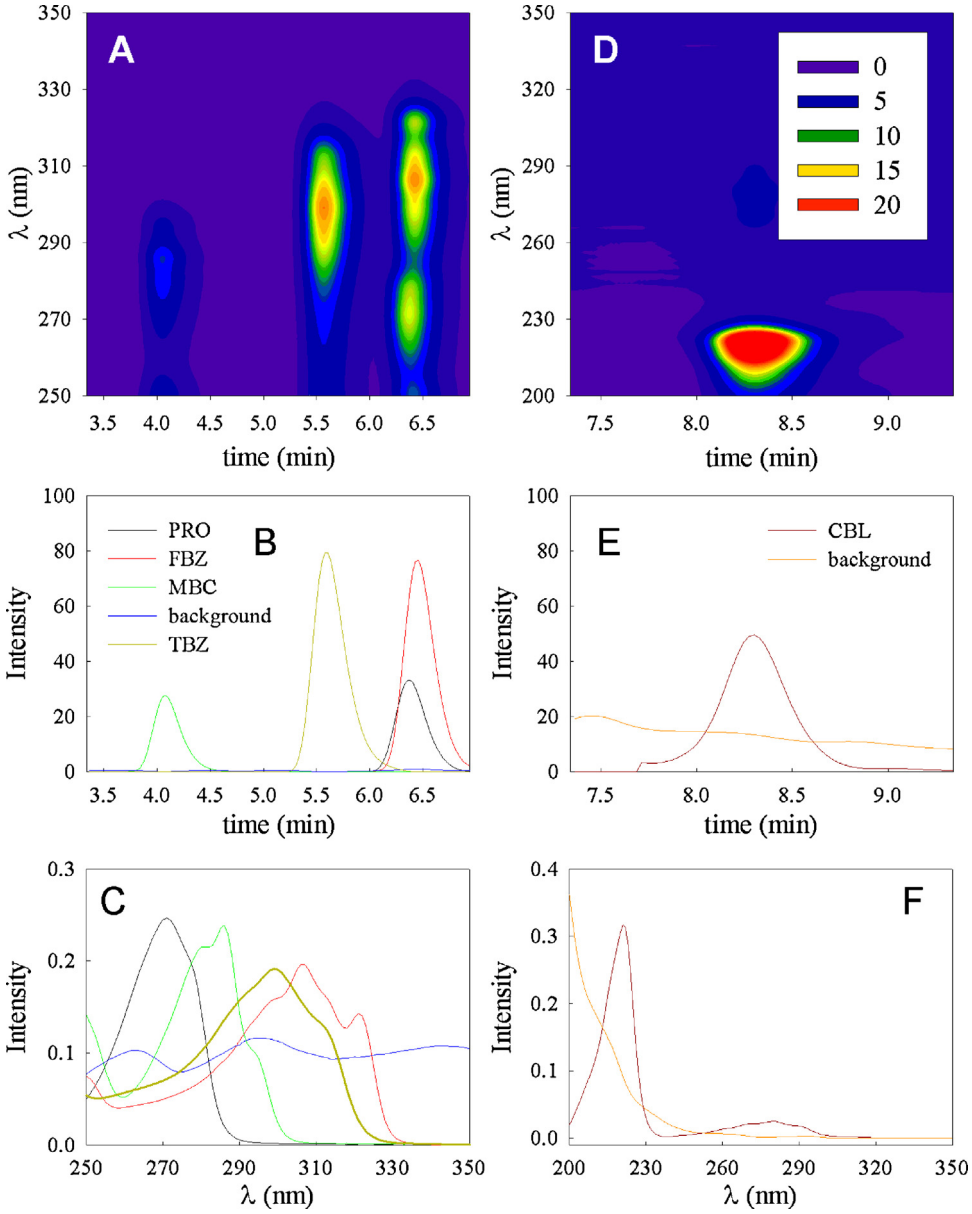

Fig. 4. Results for the analysis of a calibration sample. (A) Surface plot around the first cluster peak (region I) containing the analytes MBC, TBZ, PRO and FBZ (B) MCR–ALS resolved elution profiles for the same sample, with all analytes indicated. (C) Spectral profiles retrieved by MCR–ALS analysis, which are common to all samples. (D) Surface plot around the region II containing CBL (E) MCR–ALS resolved elution profiles in region II. (F) Spectral profiles retrieved by MCR–ALS analysis.

Table 3
MCR–ALS results for the prediction of the studied analytes in the validation set of samples.

Sample	MBC (μg L^{-1})		TBZ (μg L^{-1})		PRO (μg L^{-1})		FBZ (μg L^{-1})		CBL (μg L^{-1})	
	N	*P*[a]	*N*	*P*[a]	*N*	*P*[a]	*N*	*P*[a]	*N*	*P*[a]
1	173.0	170 (6)	95.2	87.1 (2)	963	920 (30)	9.9	10 (2)	12.2	11.3 (7)
2	166.0	165 (4)	137.0	136 (3)	1030	1070 (10)	82.3	81 (4)	121.0	123 (3)
3	0.0	1.1 (2)	149.0	146.7 (4)	602	570 (10)	32.7	31 (3)	70.7	69 (2)
4	228.0	234 (7)	53.8	51 (2)	1340	1240 (60)	21.8	21 (2)	96.6	94 (2)
5	160.0	157 (5)	164.0	158 (3)	1170	1160 (10)	71.4	71 (4)	132.0	125 (2)
6	77.5	75.8 (4)	51.8	54.2 (2)	1100	1100 (10)	36.7	36.1 (4)	44.9	46.1 (9)
7	22.8	24 (2)	176.0	185 (2)	1340	1360 (10)	45.6	44.6 (4)	46.2	47.7 (6)
8	166.0	166 (5)	74.5	73 (2)	654	603 (8)	0.9	–	89.8	88 (2)
9	185.0	188 (5)	20.7	15.7 (1)	1200	1180 (20)	13.9	13 (2)	20.4	20.5 (9)
10	66.1	66 (2)	186.0	185.8 (3)	361	340 (10)	54.6	55 (3)	6.8	6 (2)
RMSEP	2.6		4.7		43		0.85		2.6	
REP (%)	2.1		4.3		4.4		2.3		4.0	
LOD	2.3		0.90		12		0.46		0.32	
LOQ	6.9		2.7		36		1.4		1.1	
Sensitivity	0.092		0.24		0.018		0.47		1.2	
Selectivity	0.53		0.29		0.69		0.31		0.73	
Analytical sensitivity	1.4		3.7		0.28		7.2		2.9	

[a] Standard deviation in parenthesis; *N* = nominal, *P* = predicted.

traditional method of area measurements and by applying MCR–ALS to the sub-matrix containing its isolated peak. There were not significant differences between the results obtained in both ways ($p = 0.337$). Fig. 4D–F show the contour plot, the chromatogram and spectrum corresponding to this region.

4.2. Analysis of the validation set

As indicated above, data matrices were analyzed by creating augmented matrices with sub-matrices corresponding to specific time and wavelength windows (regions I and II). For quantifying the analytes in the validation set of samples, each validation

Table 4
MCR–ALS results for the prediction of the studied analytes in the spiked samples.

	Sample	MBC (μg L^{-1})		TBZ (μg L^{-1})		PRO (μg L^{-1})		FBZ (μg L^{-1})		CBL (μg L^{-1})	
		N	*P*[a]	*N*	*P*[a]	*N*	*P*[a]	*N*	*P*[a]	*N*	*P*[a]
Orange Juice	1	185.0	195 (4)	16.6	15.9 (7)	1170	1310 (20)	79.4	72.2 (7)	5.7	6.91 (7)
	2	73.0	80 (3)	10.4	12.2 (7)	48	57 (1)	30.8	28.1 (4)	88.4	97 (1)
	3	11.4	15 (3)	47.6	43.1 (8)	860	940 (10)	34.7	35.3 (4)	42.2	48.6 (6)
	4	153.0	145 (5)	93.1	84 (2)	22	36 (2)	12.9	8.1 (3)	15.0	16.2 (8)
	MRL	200		5000		50		50		10	
	RMSEP	7.6		5.2		81		4.5		5.4	
	REP (%)	6.6		4.9		9.2		8.9		8.0	
Grapefruit	5	210.0	218 (6)	76.6	72 (4)	1030	1080 (20)	41.7	44 (1)	135.0	132 (6)
Juice	6	198.0	191 (5)	201.0	205 (8)	69	53 (4)	14.9	11.8 (6)	6.8	7.9 (3)
	7	155.0	163 (5)	153.0	160 (6)	1720	1810 (40)	77.4	81 (2)	16.3	12.2 (6)
	8	25.1	20.1 (9)	64.2	70 (3)	34	37 (3)	45.6	42 (2)	105.0	101 (4)
	MRL	200		5000		50		50		10	
	RMSEP	7.2		5.5		52		3.2		3.1	
	REP (%)	6.4		5.1		5.8		6.3		4.6	
Lemon	9	160.0	151 (3)	80.7	75 (2)	224	250 (10)	14.9	15.5 (4)	40.8	38.8 (9)
	10	66.1	70 (2)	97.3	103 (3)	172	180 (10)	68.4	71 (1)	72.1	75 (2)
	11	228.0	239 (5)	132.0	136 (3)	1690	1670 (20)	71.4	69 (1)	69.4	64 (2)
	12	29.6	30.1 (6)	82.8	79 (2)	654	690 (20)	48.6	50.5 (8)	6.8	7.5 (7)
	MRL	700		5000		300		50		10	
	RMSEP	7.2		4.8		44		2.0		3.2	
	REP (%)	6.4		4.5		5.0		4.0		4.8	
Tangerine	13	132.0	125 (3)	159.0	150 (10)	1100	1070 (20)	5.9	5.2 (1)	132.0	125 (2)
	14	198.0	204 (5)	97.3	102 (5)	1200	1140 (20)	20.8	19 (1)	15.0	12.1 (2)
	15	93.5	97 (2)	207.0	200 (20)	430	440 (10)	87.3	83 (1)	80.2	78 (1)
	16	59.3	64 (2)	132.0	126 (6)	155	125 (7)	41.7	47 (2)	6.8	6.6 (3)
	MRL	700		5000		300		50		10	
	RMSEP	5.4		7.1		39		3.6		3.9	
	REP (%)	4.8		6.7		4.4		7.0		5.8	
Tomato	17	38.8	42 (1)	84.9	87.6 (9)	206	166 (4)	21.8	29.6 (4)	124.0	131 (3)
	18	80.9	76 (2)	97.3	91 (1)	1010	970 (10)	25.8	23.5 (3)	8.2	9.8 (2)
	19	108.0	115 (2)	128.0	121 (1)	740	797 (8)	60.5	56.9 (7)	59.8	65 (2)
	20	213.0	203 (3)	15.5	21.3 (7)	17	38 (7)	40.0	43.6 (6)	24.5	21 (2)
	MRL	300		50		50		50		10	
	RMSEP	6.8		5.8		43		4.8		4.8	
	REP (%)	5.9		5.4		4.9		9.5		7.1	
p Value		0.389		0.206		0.794		0.439		0.694	

[a] Standard deviation in parenthesis; *N* = nominal, *P* = predicted.

HPLC–DAD data matrix was divided into the two selected regions. For each time region, a time mode augmented matrix was created. Each augmented matrix contained, adjacent to each other, the sub-matrices corresponding to the validation samples and to the calibration samples. As before, non-negativity in both modes and unimodality in the time mode (but not correspondence) were applied during ALS optimization. Unimodality was only applied to the signal corresponding to the analytes but not to the background signals. After optimization with the multivariate algorithm, the scores corresponding to each analyte in each validation sample were isolated, and prediction proceeded by interpolation into the pseudo-univariate score-concentration calibration plot. Linear relationships between MCR–ALS scores and nominal concentrations were found in all cases, supported by the linearity test recommended by IUPAC [39]. The statistical results when MCR–ALS was applied to this validation set are shown in Table 2, implying linearity for all analytes.

As can be observed in Table 3, the predictions for the five analytes are in good agreement with the corresponding nominal values. The root mean square error of prediction (RMSEP) and the relative errors of prediction (REP), computed with respect to the mean calibration concentration of each analyte, can be calculated as follows:

$$\mathrm{RMSEP} = \sqrt{\frac{\sum_{t=1}^{T}\left(y_{\mathrm{pred},t} - y_{\mathrm{nom},t}\right)^2}{T}} \tag{6}$$

$$\mathrm{REP} = 100\frac{\mathrm{RMSEP}}{\bar{y}_{\mathrm{cal}}} \tag{7}$$

where $y_{\mathrm{pred},t}$ is the predicted concentration in each sample, $y_{\mathrm{nom},t}$ is the nominal value of the concentration in the sample, T is the number of test samples, and $\bar{y}_{\mathrm{cal}}$ is the mean calibration concentration. The RMSEP and REP values are also quoted in Table 3. The

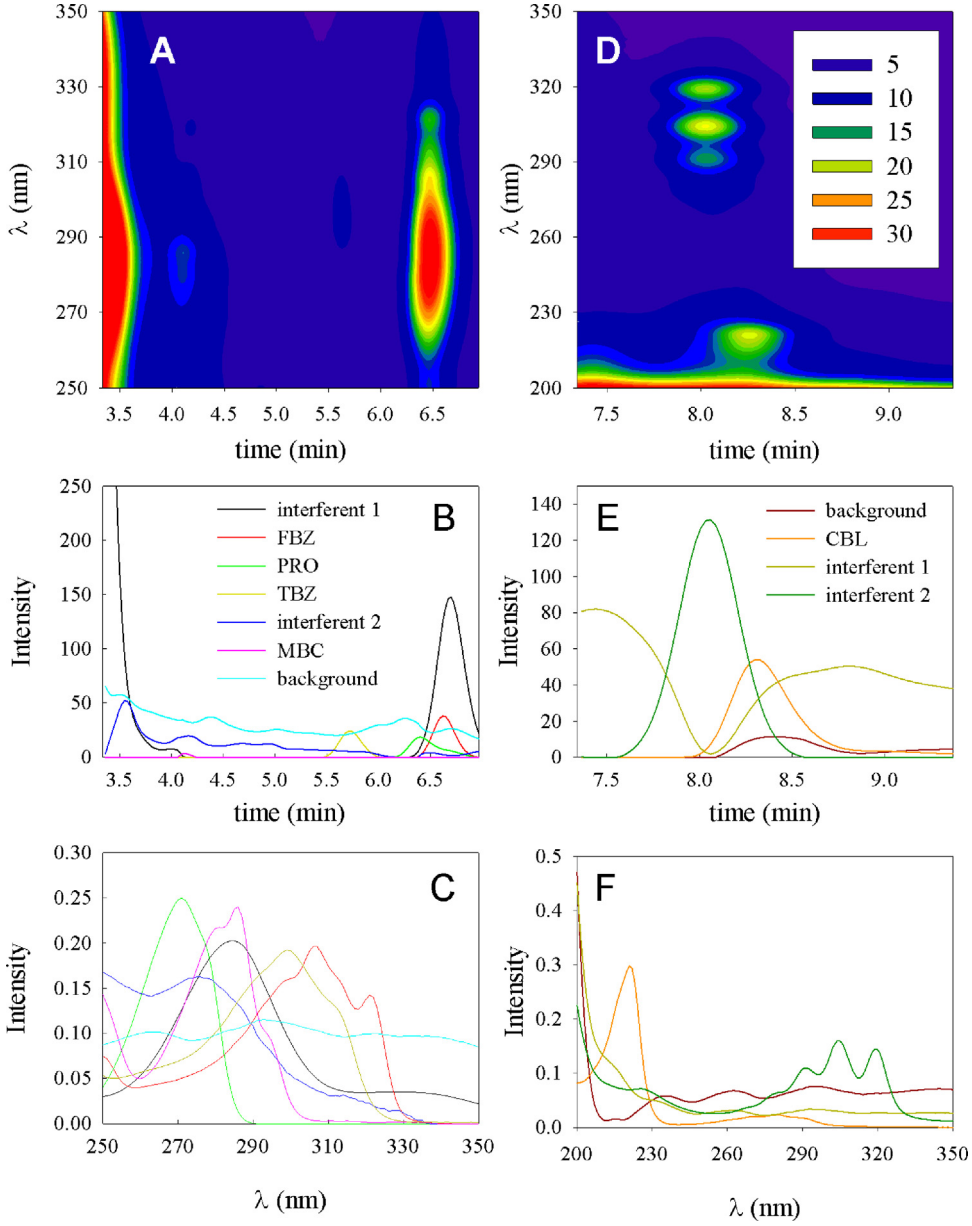

Fig. 5. Results for the analysis of an orange juice sample. (A) Surface plot around the first cluster peak (region I) containing the analytes MBC, TBZ, PRO and FBZ (B) MCR–ALS resolved elution profiles for the same sample, with all analytes indicated. (C) Spectral profiles retrieved by MCR–ALS analysis. (D) Surface plot around the region II containing CBL (E) MCR–ALS resolved elution profiles in region II. (F) Spectral profiles retrieved by MCR–ALS analysis.

limits of detection (LOD) and limits of quantification (LOQ) were calculated taking into account the errors of the slope and intercept of the pseudo-univariate calibration curves, as was previously reported by Saurina et al. [40].

4.3. Analysis of spiked real samples

Official regulating agencies recommend maximum residue levels (MRL) for the presently studied pesticides which are listed in Table 4 for the assayed fruits and vegetables samples. As can be seen, these values are higher than the calculated LOD (Table 3), and thus analyte pre-concentration is not required.

Real fruit and vegetable samples were spiked with these five pesticides and were subjected to the analytical protocol discussed above. The estimated number of components was seven or eight in region I and four in region II, i.e., there are additional components in comparison to the calibration and validation samples. Therefore, the analysis of these samples revealed that there are various interfering species in each region, depending on the sample.

Each data matrix was divided into the two selected regions. As before, non-negativity in both modes and unimodality in the time mode were applied during ALS optimization. Unimodality was only applied to the signal corresponding to the analytes but not to the background signals or to the signals corresponding to interferents. In fact, some of the signals corresponding to interferents have more than one maximum in the time mode. This may be indicating that the interferents are not unique compounds, but also a combination of compounds with similar UV spectra that cannot be resolved by MCR. As regards the correspondence restriction (which informs MCR–ALS that the potential interferents are absent in the calibration samples), it is interesting that there was no significant difference when applying correspondence or when this restriction was not applied. The number of iterations was less than 100 in all cases, with a residual fit lower than 0.3 mUA (region I) and 0.45 mUA (region II).

Fig. 5A–F shows the contour plot, the chromatogram and spectrum corresponding to both regions for one sample of orange juice. As can be seen, the spectra corresponding to the interfering species were different to those corresponding to the pesticides, allowing their resolution. The recovery results corresponding to different levels of each pesticide the five type of sample assayed are collected in Table 4. As can be appreciated, the predictions for the analytes are in good agreement with the nominal values. If the elliptical joint confidence region is analyzed for the slope and intercept of plot of predicted vs. nominal concentrations we conclude that the ellipse includes the theoretically expected values of (1,0), indicating the accuracy of the used methodology (data not shown). Indeed, a paired *t*-test indicates no significant difference between the nominal concentrations and the predicted using the presently proposed methodology. The *p* values are also listed in Table 4. This strongly suggests that HPLC–DAD combined to MCR–ALS is a useful methodology for the analysis of these pesticides in commercial juices, fruit and vegetable samples.

5. Conclusions

Complex samples including strongly coeluting analytes, elution time shifts, band shape changes and presence of uncalibrated interferents have been analyzed by HPLC–DAD. The flexibility of the applied multivariate model (MCR–ALS) allows the prediction of the concentrations of five analytes in a set of validation samples. More importantly, in the most challenging analytical scenario, i.e., real vegetable and fruit samples, these five analytes were quantified within a coeluting cluster in the presence of unwanted and non calibrated signals, achieving the second-order advantage which is inherent to second-order HPLC–DAD information.

Acknowledgments

Financial support provided by the University of Rosario, CONICET and ANPCyT (Project No. PIP 2010-0084) is appreciated. Valeria Boeris is grateful to CONICET for her scholarship.

References

[1] S. Topuz, G. Özhan, B. Alpertunga, Food Control 16 (2005) 87–92.
[2] European Commission, ⟨http://ec.europa.eu/⟩, last accessed on 24th January 2014.
[3] U.S. Department of Health & Human Services. U.S. Food and Drug Administration, ⟨http://www.fda.gov/⟩, last accessed on 24th January 2014.
[4] G.F. Pang, C.L. Fan, Y.M. Liu, Y.Z. Cao, J.J. Zhang, B.L. Fu, X.M. Li, Z.Y. Li, Y.P. Wu, Food Addit. Contam. 23 (2006) 777–810.
[5] A. Bordagaray, R. Garcia-Arrona, E. Millan, Anal. Methods 5 (2013) 2565–2571.
[6] X.Y. Song, Y.P. Shi, J. Chen, Food Chem. 139 (2013) 246–252.
[7] G. Rübensam, F. Barreto, R.B. Hoff, T.M. Pizzolato, Food Control 29 (2013) 55–60.
[8] C. Carrillo-Carrión, B.M. Simonet, M. Valcárcel, Anal. Chim. Acta 692 (2011) 103–108.
[9] A. Moral, M.D. Sicilia, S. Rubio, Anal. Chim. Acta 650 (2009) 207–213.
[10] G.E. Mercer, J.A. Hurlbut, J. AOAC Int. 87 (2004) 1224–1236.
[11] R.J. Bushway, D.L. Brandon, A.H. Bates, L. Li, K.A. Larkin, B.S. Young, J. Agric. Food Chem. 43 (1995) 1407–1412.
[12] G.S. Nunes, M.P. Marco, M. Farré, D. Barceló, Anal. Chim. Acta 387 (1999) 245–253.
[13] J. Sun, T. Dong, Y. Zhang, S. Wang, Anal. Chim. Acta 666 (2010) 76–82.
[14] G.S. Nunes, D. Barceló, B.S. Grabaric, J.M. Dı′az-Cruz, M.L. Ribeiro, Anal. Chim. Acta 399 (1999) 37–49.
[15] J. Caetano, S.A.S. Machado, Sens. Actuators, B 129 (2008) 40–46.
[16] Q. Wu, Q. Chang, C. Wu, H. Rao, X. Zeng, C. Wang, Z. Wang, J. Chromatogr. A 1217 (2010) 1773–1778.
[17] S. Broecker, F. Pragst, A. Bakdash, S. Herre, M. Tsokos, Forensic Sci. Int. 212 (2011) 215–226.
[18] M.J. Rodrı′guez-Cuesta, R. Boqué, F.X. Rius, D. Picón Zamora, M. Martı′nez Galera, A. Garrido Frenich, Anal. Chim. Acta 491 (2003) 47–56.
[19] M.J. Rodríguez-Cuesta, R. Boqué, F.X. Rius, J.L. Martínez Vidal, A. Garrido Frenich, Chemom. Intell. Lab. Syst. 77 (2005) 251–260.
[20] X.D. Qing, H.L. Wu, C.C. Nie, X.F. Yan, Y.N. Li, J.Y. Wang, R.Q. Yu, Talanta 103 (2013) 86–94.
[21] R.M. Maggio, P.C. Damiani, A.C. Olivieri, Talanta 83 (2011) 1173–1180.
[22] S.A. Bortolato, J.A. Arancibia, G.M. Escandar, Anal. Chem. 80 (2008) 8276–8286.
[23] K.S. Booksh, B.R. Kowalski, Anal. Chem. 66 (1994) 782A–791A.
[24] H. Obana, M. Okihashi, K. Akutsu, Y. Kitagawa, S. Hori, J. Agric. Food Chem. 50 (2002) 4464–4467.
[25] S. Seccia, S. Albrizio, P. Fidente, D. Montesano, J. Chromatogr. A 1218 (2011) 1253–1259.
[26] M. Saraji, N. Tansazan, J. Sep. Sci. 32 (2009) 4186–4192.
[27] Y. Zhou, G. Xu, F.F.K. Choi, L.S. Ding, Q.B. Han, J.Z. Song, C.F. Qiao, Q.S. Zhao, H.X. Xu, J. Chromatogr. A 1216 (2009) 4847–4858.
[28] A. Belmonte Vega, A. Garrido Frenich, J.L. Martínez Vidal, Anal. Chim. Acta 538 (2005) 117–127.
[29] M. Fernández, Y. Picó, J. Mañes, J. Chromatogr. A 871 (2000) 43–56.
[30] J. Jaumot, R. Gargallo, A. de Juan, R. Tauler, Chemom. Intell. Lab. Syst. 76 (2005) 101–110.
[31] M. Maeder, A. Zilian, Chemom. Intell. Lab. Syst. 3 (1988) 205–213.
[32] M. Maeder, Anal. Chem. 59 (1987) 527–530.
[33] W. Windig, J. Guilment, Anal. Chem. 63 (1991) 1425–1432.
[34] G.H. Golub, C.F. Van Loan, Matrix Computations, Johns Hopkins University Press, Baltimore, MD, 1996.
[35] R. Tauler, A. Smilde, B. Kowalski, J. Chemom. 9 (1995) 31–58.
[36] R. Tauler, M. Maeder, A. de Juan, Multiset data analysis: extended multivariate curve resolution, in: S.D. Brown, R. Tauler, B. Walczak (Eds.), Comprehensive Chemometrics, Elsevier, Oxford, 2009, pp. 473–505.
[37] MATLAB version 2011b, The Mathworks Inc., Natick, MA.
[38] A.C. Olivieri, H.L. Wu, R.Q. Yu, Chemom. Intell. Lab. Syst. 96 (2009) 246–251.
[39] K. Danzer, L.A. Currie, Pure & Appl. Chem. 70 (1998) 993–1014.
[40] J. Saurina, C. Leal, R. Compañó, M. Granados, M.D. Prat, R. Tauler, Anal. Chim. Acta 432 (2001) 241–251.